報告のように手技の工夫や経験で改善させることは可能で，今回の症例でも幸い再手術後は全例に骨癒合を獲得でき，最終的な神経症状の改善は良好であった．また，neuropathic pain などの難治性疼痛は椎弓形成術の 8%に認められ疼痛管理に難渋しているが，前方法では外傷後の 1 例(症例 2)を除いて認めていない．

今後経過観察を伸ばし詳細な比較検討が必要ではあるが，1)占拠率 60%以上の大きな骨化症，2)局所的脊髄圧迫(山型の骨化パターン)，3)頚椎不良アライメントあるいは動的因子が関与する症例では，患者・医師とも合併症を許容できれば前方除圧固定術(骨化摘出または骨化浮上)を選択していくことが治療成績向上につながるものと考える．

結 論

頚椎 OPLL に対する術式選択は，骨化占拠率・骨化形態や矢状面骨化パターン・頚椎アライメント・骨化間や椎間での可動性・患者年齢・術者の経験と技術を考慮して決定していく必要がある．骨化占拠率 60%以上の大きい骨化や山型の骨化パターンおよび不良アライメントの症例は椎弓形成術の限界と考えられ，治療成績の向上を期待し合併症を許容できれば前方法を選択すべきである．

本論文の要旨は第 77 回日本整形外科学会学術集会(2004 年 5 月　神戸)，第 33 回日本脊椎脊髄病学会(2004 年 6 月　東京)，第 35 回日本脊椎脊髄病学会(2006 年 4 月　東京)，第 79 回日本整形外科学会学術集会(2006 年 5 月　横浜)にて発表した．

文　献

1) Belanger TA, Roh JS, Hanks SE, et al：Ossification of the posterior longitudinal ligament. Results of anterior cervical decompression and arthrodesis in sixty-one North American patients. J Bone Joint Surg Am **87**：610-615, 2005
2) Chiba K, Yamamoto I, Hirabayashi H, et al：Multicenter study investigating the postoperative progression of ossification of the posterior longitudinal ligament in the cervical spine：a new computer-assisted measurement. J Neurosurg Spine **3**：17-23, 2005
3) Epstein N：The surgical management of ossification of the posterior longitudinal ligament in 51 patients. J Spinal Disord **6**：432-454, 1993
4) 平林　洌：頚髄症に対する後方除圧法としての片開き式頚部脊柱管拡大術について．手術 **32**：1159-1163, 1978
5) Hirabayashi K, Watanabe K, Wakano K, et al：Expansive open-door laminoplasty for cervical spinal stenotic myelopathy. Spine **8**：693-699, 1983
6) Ikenaga M, Shikata J, Tanaka C：Anterior corpectomy and fusion with fibular strut grafts for multilevel cervical myelopathy. J Neurosurg Spine **3**：79-85, 2005
7) Itoh T, Tsuji H：Technical improvements and results of laminoplasty for compressive myelopathy in the cervical spine. Spine **10**：729-736, 1985
8) Iwasaki M, Ebara S, Miyamoto S, et al：Expansive laminoplasty for cervical radiculomyelopathy due to soft disc herniation. Spine **21**：32-38, 1996
9) Iwasaki M, Kawaguchi Y, Kimura T, et al：Long-term results of expansive laminoplasty for ossification of the posterior longitudinal ligament of the cervical spine：more than 10 years follow up. J Neurosurg(Spine 2)**96**：180-189, 2002
10) 岩﨑幹季：椎弓形成術は椎弓切除術に勝るか？脊椎脊髄 **17**：232-234, 2004
11) 岩﨑幹季，奥田真也，宮内　晃：頚椎後縦靱帯骨化症に対する外科的治療戦略—後方除圧術の限界．別冊整形外科 45：197-200, 2004
12) 岩﨑幹季，宮内　晃，奥田真也・他：頚椎後縦靱帯骨化症：治療に関するシステマティックレビュー．脊椎脊髄 **19**：133-142, 2006
13) Iwasaki M：Overview of treatment for ossification of the longitudinal ligament and the ligamentum flavum. *In*：Yonenobu K, Nakamura K, Toyama Y (ed). OPLL Ossification of the Posterior Longitudinal Ligament. 2nd ed, Springer, Tokyo；165-167, 2006
14) Iwasaki M, Yonenobu K：Choice of surgical procedure. *In*：Yonenobu K, Nakamura K, Toyama Y(ed). OPLL Ossification of the Posterior Longitudinal Ligament. 2nd ed Springer, Tokyo；181-185, 2006
15) Iwasaki M, Yonenobu K：Ossification of the posterior longitudinal ligament. *In*：Herkowitz HN, Garfin SR, Eismont FJ, et al(ed). Rothman-Simone The Spine. 5th ed. Elsevier, Philadelphia, 2006
16) Iwasaki M, Okuda S, Miyauchi A, et al：Surgical strategy for cervical myelopathy due to ossification of the posterior longitudinal ligament. Part 1：Clinical results and limitations of laminoplasty. Spine(in press), 2007
17) Iwasaki M, Okuda S, Miyauchi A, et al：Surgical strategy for cervical myelopathy due to ossification of the posterior longitudinal ligament. Part 2：

Advantages of anterior decompression and fusion over laminoplasty. Spine (in press), 2007
18) Kato Y, Iwasaki M, Fuji T, et al : Long-term follow-up results of laminectomy for cervical myelopathy caused by ossification of the posterior longitudinal ligament. J Neurosurg **89** : 217-223, 1998
19) Kawaguchi Y, Kanamori M, Ishihara H, et al : Progression of ossification of the posterior longitudinal ligament following en bloc cervical laminoplasty. J Bone Joint Surg Am **83** : 1798-1802, 2001
20) Matsunaga S, Kukita M, Hayashi K, et al : Pathogenesis of myelopathy in patients with ossification of the posterior longitudinal ligament. J Neurosurg **96** : 168-172, 2002
21) Matsunaga S, Sakou T, Taketomi E, et al : The natural course of myelopathy caused by ossification of the posterior longitudinal ligament in the cervical spine. Clin Orthop Relat Res **305** : 168-177, 1994
22) Ogawa Y, Toyama Y, Chiba K, et al : Long-term results of expansive open-door laminoplasty for ossification of the posterior longitudinal ligament of the cervical spine. J Neurosurg Spine **1** : 168-174, 2004
23) Shinomiya K, Okamoto A, Kamikozuru M, et al : An analysis of failures in primary cervical anterior spinal cord decompression and fusion. J Spinal Disord **6** : 277-288, 1993
24) Sodeyama T, Goto S, Mochizuki M, et al : Effect of decompression enlargement laminoplasty for posterior shifting of the spinal cord. Spine **24** : 1527-1531, 1999
25) Takeshita K, Seichi A, Akune T, et al : Can laminoplasty maintain the cervical alignment even when the C2 lamina is contained? Spine **30** : 1294-1298, 2005
26) Tani T, Ushida T, Ishida K, et al : Relative safety of anterior microsurgical decompression versus laminoplasty for cervical myelopathy with a massive ossified posterior longitudinal ligament. Spine **27** : 2491-2498, 2002
27) 寺山和雄，山岡弘明，八木　了・他：後縦靱帯骨化．整形外科 **30** : 361-369, 1979
28) 月本裕国：頚部後縦靱帯化骨により脊髄圧迫症候を呈した1剖検例．日本外科宝函 **29** : 1003-1007, 1960
29) Tsuyama N : Ossification of the posterior longitudinal ligament of the spine. Clin Orthop Relat Res **184** : 71-84, 1984
30) 山浦伊裟吉：後縦靱帯骨化症および脊柱管狭窄症に対する前方除圧法—骨化浮上術，脊柱管前方拡大術について．臨整外 **18** : 855-868, 1983
31) Yamaura I, Kurosa Y, Matuoka T, et al : Anterior floating method for cervical myelopathy caused by ossification of the posterior longitudinal ligament. Clin Orthop Relat Res **359** : 27-34, 1999
32) Yamazaki A, Homma T, Uchiyama S, et al : Morphologic limitations of posterior decompression by midsagittal splitting method for myelopathy caused by ossification of the posterior longitudinal ligament in the cervical spine. Spine **24** : 32-34, 1999
33) Yonenobu K, Wada E, Ono K : Part B. Laminoplasty. *In* : The Cervical Spine Research Society Editorial Committee (ed). The Cervical Spine. 4th ed. Lippincott Williams & Wilkins, Philadelphia ; 1057-1071, 2005

「読者の声」募集

弊誌では，読者の皆様の“ひとこと”(ご意見)を募集しています．

1) 原稿の内容については特に限定いたしませんが，以下のような内容を歓迎いたします．掲載の採否は編集委員会で決定させていただきます．

- 診療，研究のなかでのエピソード，気づいた出来事，雑感
- 弊誌掲載論文，記事などに対する感想，意見
- 整形外科臨床，整形外科学(医学)教育，整形外科臨床研修などをめぐる諸問題
- 医療行政，社会保険制度などについての感想，意見

2) ご送付の際は弊誌Eメール(rinseige@igaku-shoin.co.jp)または綴じ込みハガキをご利用ください．(レイアウトの関係で字数等多少変更させていただくことがあります．)

『臨床整形外科』編集室

An Analysis of Factors Causing Poor Surgical Outcome in Patients With Cervical Myelopathy Due to Ossification of the Posterior Longitudinal Ligament

Anterior Decompression With Spinal Fusion Versus Laminoplasty

Yutaka Masaki, MD, Masashi Yamazaki, MD, PhD, Akihiko Okawa, MD, PhD, Masaaki Aramomi, MD, Mitsuhiro Hashimoto, MD, Masao Koda, MD, PhD, Makondo Mochizuki, MD, and Hideshige Moriya, MD, PhD

Objective: We compared the surgical outcome of anterior decompression with spinal fusion (ASF) with the surgical outcome of laminoplasty for patients with cervical myelopathy due to ossification of the posterior longitudinal ligament.

Methods: The study group comprised 19 ASF patients (A-group) and 40 laminoplasty patients (P-group) treated from 1993 to 2002 with 1 year or longer follow-up. The Japanese Orthopedic Association scoring system was used to evaluate cervical myelopathy, and the recovery rate calculated 1 year after surgery.

Results: The mean recovery rate was 68.4% in the A-group and 52.5% in the P-group ($P < 0.05$). Fifteen patients had a recovery rate less than 40%: 2 in the A-group and 13 in the P-group. One P-group patient and none of the A-group patients developed postoperative aggravation of their neurologic status. The P-group was divided into 2 subgroups: a good outcome group comprising patients whose recovery rate was 40% or higher (n = 27) and a poor outcome group comprising patients whose recovery rate was less than 40% (n = 13). The mean age at surgery was 59.9 years in the good outcome group and 68.0 years in the poor outcome group ($P < 0.05$). The mean range of intervertebral mobility at maximum cord compression level before surgery was 6.9 degrees in the good outcome group and 10 degrees in the poor outcome group ($P < 0.05$).

Conclusions: These results demonstrated that the surgical outcome of ASF was superior to the surgical outcome of laminoplasty. Elderly patients treated with laminoplasty showed an especially poor surgical outcome. We suggest that hypermobility of vertebrae at the cord compression level is a risk factor for poor surgical outcome after laminoplasty. Based on these results, we recommend that ASF should be the first choice of treatment for patients with significant ossification of the posterior longitudinal ligament and a hypermobile cervical spine. When laminoplasty is used for such cases, the addition of posterior instrumented fusion would be desirable for stabilizing the spine and decreasing damage to the spinal cord.

Key Words: ossification of posterior longitudinal ligament, cervical myelopathy, anterior decompression with spinal fusion, laminoplasty

(*J Spinal Disord Tech* 2007;20:7–13)

Heterotopic ossification of the posterior longitudinal ligament (OPLL) leads to narrowing of the spinal canal. In the Japanese population, extensive ossification often develops in the spinal ligaments, including the posterior longitudinal ligament.[1] OPLL consequently represents one of the most common causes of cervical myelopathy in Japan, along with disc herniation and spondylosis.[1] Because conservative treatment is usually ineffective for severe myelopathy caused by OPLL, surgical treatment is chosen in most cases. Decompressive surgical procedures for OPLL-related cervical myelopathy can be divided into those using an anterior approach and those using a posterior approach. Several reports have analyzed the surgical outcomes of anterior and posterior surgeries; however, evaluation of the surgical procedures differs between institutions.[2–13] Furthermore, guidelines for selecting surgical procedures for cervical OPLL have not yet been fully established.

Since 1968, we have performed surgery using anterior or posterior approaches for patients with cervical myelopathy due to OPLL.[6] Between 1968 and 1991, we have twice modified the procedures of our anterior and posterior surgeries. During the first phase, from 1968 to 1980, we performed anterior decompression with spinal

Received for publication April 30, 2006; accepted July 24, 2006.
From the Department of Orthopaedic Surgery, Chiba University Graduate School of Medicine, 1-8-1 Inohana, Chuo-ku, Chiba 260-8677, Japan.
Supported by a Grant-in-Aid for Scientific Research from the Ministry of Education, Culture, Sports, Science and Technology of Japan, and by a Grant for Intractable Diseases from the Public Health Bureau, the Ministry of Health, Labour and Welfare of Japan (Investigation Committee on Ossification of the Spinal Ligaments).
Reprints: Masashi Yamazaki, MD, PhD, Department of Orthopaedic Surgery, Chiba University Graduate School of Medicine, 1-8-1 Inohana, Chuo-ku, Chiba 260-8677, Japan (e-mail: masashiy@faculty.chiba-u.jp).

TABLE 1. Summary of Clinical Data for the 59 Study Cases

Surgical Groups	A-group Anterior Decompression and Fusion	P-group Laminoplasty
Total cases	19	40
Sex		
Males	14	30
Females	5	10
Age at surgery (y)*	51.8 ± 6.6 (39-64)	62.6 ± 10.3‡ (38-82)
Duration of symptoms (mo)*	29.1 ± 41.2 (1-161)	50.0 ± 43.3† (3-136)
No. ossified vertebra*	2.5 ± 1.1 (2-6)	4.1 ± 1.3‡ (2-6)
OPLL occupation ratio (%)*	56.0 ± 8.0 (45.5-72.7)	55.9 ± 14.3 (20-90)
No. operated segments*	2.9 ± 0.9 (1-4)	4.6 ± 0.5‡ (4-5)

*The values are expressed as the mean ± standard deviation, with the range in parentheses.
†Statistically different from the data in A-group ($P < 0.05$).
‡Statistically different from the data in A-group ($P < 0.01$).

fusion (ASF) and extirpation of OPLL within 3 intervertebral disc levels below C4 as the anterior procedure, and laminectomy for multilevel lesions over 3 intervertebral disc levels as the posterior procedure. During the second phase, from 1980 to 1986, we modified our anterior procedure by extending ASF up to 3 intervertebral disc levels below C3, and replaced laminectomy with laminoplasty as our posterior procedure. During the third phase, from 1986 to 1991, we further modified the anterior procedure by using a cervical distractor and intraoperative ultrasonography, and modified the posterior procedure by incorporating domelike enlargement of the C2 lamina and extirpation of the C1 posterior arch when necessary. In cases with anterior surgery, the first and second modifications of surgical techniques have improved neurologic recovery, respectively. Similar improvement was also observed in cases with posterior surgery. Our recent follow-up studies of cases during our third phase found that the surgical outcome of ASF was superior to that of laminoplasty; the mean recovery rate after ASF was 71.4% and that after laminoplasty was 61.4%, indicating that complete decompression of the spinal cord anteriorly may result in better neurologic recovery than indirect decompression posteriorly.[6]

Starting in 1993, we presented the recent surgical outcome and the standardized informed consent of both anterior and posterior surgeries to all cervical OPLL patients who were scheduled to undergo surgery at our institute. We selected the surgical approach in accordance with the patients' choice between anterior and posterior surgeries. In the present study, we compared the results of anterior and posterior surgeries performed after 1993, and we analyzed factors related to poor surgical outcomes.

MATERIALS AND METHODS

Patient Population

From June 1993 to July 2002, 66 patients with cervical myelopathy due to OPLL underwent surgical treatment (21 anterior, 45 posterior) at our institute. Of these 66 patients, 7 patients (2 anterior, 5 posterior) were excluded from this study because they had undergone follow-up evaluation of less than 1 year duration. The study group thus comprised the remaining 19 anterior surgery patients (A-group) and 40 posterior surgery patients (P-group) with 1 year or longer follow-up after surgery, a total of 59 patients (44 males and 15 females). Their mean age at surgery was 59.4 years, ranging from 38 to 82 years (Table 1).

Selection Between Anterior and Posterior Surgery

Before surgery, we provided standardized informed consent to all cervical OPLL patients who were scheduled to have surgery in our institute. We explained our recent surgical results of both ASF and laminoplasty to the patients, including neurologic recovery, surgery-related complications, and postoperative neck immobilization with a cervical orthosis. We selected the surgical approach in accordance with the patients' choice between anterior and posterior surgery.

We explained the relative advantages of anterior surgery (ASF) as follows: (1) excision of the ossified mass enables complete decompression of the spinal cord; (2) ASF creates a solid spinal fusion that can relieve pressure on the injured spinal cord. We also discussed the following disadvantages of ASF compared with laminoplasty: (1) more skillful techniques are required for ASF than for laminoplasty; (2) harvesting the graft bone from the iliac crest or fibula entails a risk of additional complications, such as donor site pain; (3) ASF requires a longer postoperative immobilization of the neck with a cervical orthosis; and (4) ASF is principally not applicable to the lesion above C2 and below T3.[6,7,10,12]

We also explained the relative advantages of posterior surgery (laminoplasty) as follows: (1) the surgical technique is less difficult for laminoplasty than for ASF; (2) the duration of hospitalization and postoperative immobilization of the neck with an orthosis is shorter for laminoplasty than for ASF. We also discussed the following disadvantages of laminoplasty compared with ASF: (1) decompression of the spinal cord after laminoplasty occurs by a posterior shift of the cord, that is, by so-called indirect decompression. If the posterior shift is not enough, anterior compression of the cord by

TABLE 2. The JOA Scoring System for Cervical Myelopathy

Score (Points)	Categories
	Motor function
	Fingers
0	Unable to feed oneself w/any tableware including chopsticks, spoon, or fork, &/or unable to fasten buttons of any size
1	Can manage to feed oneself w/spoon &/or fork but not w/chopsticks
2	Either chopstick feeding or writing is possible but not practical, &/or large buttons can be fastened
3	Either chopstick feeding or writing is clumsy but practical, &/or cuff buttons can be fastened
4	Normal
	Shoulder & elbow: evaluated by MMT score of delotoid or biceps muscles, whichever is weaker
−2	MMT 2 or below
−1	MMT 3
−0.5	MMT 4
0	MMT 5
	Low extremity
0	Unable to stand up & walk by any means
0.5	Able to stand up but unable to walk
1	Unable to walk w/out a cane to other support on a level
1.5	Able to walk w/out support but w/a clumsy gait
2	Walks independently on a level but needs support on stairs
2.5	Walks independently when going upstairs, but needs support when going down stairs
3	Capable of fast walking but clumsily
4	Normal
	Sensory function
	Upper extremity
0	Complete loss of touch & pain sensation
0.5	≤50% normal sensation &/or severe pain or numbness
1	≥60% normal sensation &/or moderate pain or numbness
1.5	Subjective numbness of a slight degree w/out any objective sensory deficit
2	Normal
	Trunk
0	Complete loss of touch & pain sensation
0.5	≤50% normal sensation &/or severe pain or numbness
1	≥60% normal sensation &/or moderate pain or numbness
1.5	Subjective numbness of as light degree w/out any objective sensory deficit
2	Normal
	Low extremity
0	Complete loss of touch & pain sensation
0.5	≤50% normal sensation &/or severe pain or numbness
1	≥60% normal sensation &/or moderate pain or numbness
1.5	Subjective numbness of as light degree w/out any objective sensory deficit
2	Normal
	Bladder function
0	Urinary retention &/or incontinence
1	Sensory of retention &/or dribbling &/or thin stream &/or incomplete continence
2	Urinary retardation &/or pollakiuria
3	Normal

Full score = 17 points.
Recovery rate = (postoperative score − preoperative score/full score − preoperative score) × 100.
MMT indicates manual muscle test.

the ossified mass may persist, leading to diminished recovery from myelopathy; (2) the frequency of postoperative neck pain due to injury to the nuchal muscles is generally higher after laminoplasty than after ASF.[2,6,8,11,13]

Surgical Techniques

Our anterior surgery procedure (ASF) has been described in detail previously.[6] The area of decompression and spinal fusion varies from a single intervertebral disc level to 4 intervertebral disc levels. We normally perform complete excision of the ossified mass, but when cerebrospinal fluid leakage and/or massive bleeding occurs during excision of the OPLL, we intraoperatively alter the procedure to the anterior floating method, in which the OPLL is incompletely removed, leaving behind a thin layer of OPLL on the reexpanded dura.[7,10] Spinal fusion is performed with an autogenious iliac crest or fibula bone graft. Internal fixation devices such as a plate and screw system normally are not used.

Our posterior surgery procedure is cervical enlargement laminoplasty, normally consisting of a C3-C7 en-block laminoplasty (Itoh's method).[3] Depending on the degree of cord compression, we sometimes add C2 dome laminotomy, resection of C1 posterior arch, and/or laminoplasty of T1.

Postoperatively, patients are allowed to sit up wearing a cervical orthosis within the first week after

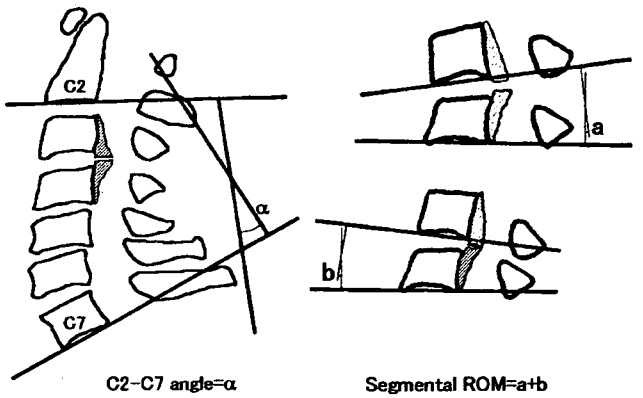

FIGURE 1. Measurements of the cervical lordotic angle (C2-C7 angle) on a lateral radiograph and the range of intervertebral mobility at the maximum cord compression level (segmental range of motion) on extension and flexion radiographs. The C2-C7 angle = α, the segmental range of motion = a+b.

surgery. After an ASF of 1to 3 intervertebral disc levels, patients wear a molded cervicothoracic orthosis for 2 months and then a soft cervical collar for 1 month. After an ASF of four intervertebral levels (3-level corpectomy), patients are cared for in the intensive care unit with intratracheal tubing for the first 48 hours after surgery, and they wear a Halo-vest for at least 2 months. After laminoplasty, patients wear a molded cervicothoracic orthosis or a soft cervical collar for 1 to 3 months after surgery.

Clinical Assessment

The Japanese Orthopedic Association (JOA) scoring system was used to evaluate the severity of cervical myelopathy (Table 2). The JOA scores before surgery and 1 year after surgery were evaluated, and the recovery rate was calculated. We defined the surgical outcome as follows: excellent (80% ≤ recovery rate), good (40% ≤ recovery rate < 80%), fair (10% ≤ recovery rate < 40%), unchanged (0% ≤ recovery rate 10%), or worsened (recovery rate < 0%).

Radiographic Assessment

Extension and flexion radiographs were assessed before surgery and 1 year after surgery, and were used to measure the range of intervertebral mobility at the level of maximum spinal cord compression (segmental range of motion) (Fig. 1). The cervical lordotic angle (C2-C7 angle) was measured on lateral radiographs before surgery and 1 year after surgery (Fig. 1), and the change of cervical lordosis was calculated as follows: ΔC2-C7 lordotic angle = C2-C7 angle after surgery-C2-C7 angle before surgery. All patients had computed tomography before surgery, and the occupation ratio of the ossified mass at the most stenotic level of the spinal canal was defined as follows: OPLL occupation ratio = (thickness of OPLL/anteroposterior diameter of the bony spinal canal) × 100.

Statistical Analysis

The Mann-Whitney *U* test was used for unpaired data. *P* values < 0.05 were considered significant. Results are presented as the mean ± standard deviation of the mean.

RESULTS

Anterior Surgery Versus Posterior Surgery

Preoperative clinical data for the A-group and the P-group are summarized in Table 1. The mean age at surgery was 51.8 years for the A-group and 62.6 years for the P-group, indicating that at the time of surgery, the laminoplasty patients were significantly older than the ASF patients ($P < 0.01$). The duration of symptoms (the period from the onset of myelopathy until surgery) was significantly longer for the laminoplasty patients: 29.1 months for the A-group vs. 50.0 months for the P-group ($P < 0.05$). The mean number of ossified vertebra was 2.5 in the A-group and 4.1 in the P-group ($P < 0.01$). The OPLL mean occupation ratio in the spinal canal did not significantly differ between the 2 groups: 56.0% for the A-group versus 55.9% for the P-group.

TABLE 3. Clinical Results of Surgery for the 59 Study Cases

Surgical Groups	A-group Anterior Decompression and Fusion (n = 19)	P-group Laminoplasty (n = 40)
JOA score (points)*		
Before surgery	8.3 ± 2.9 (4-12)	8.6 ± 2.4 (2-12)
After surgery	14.2 ± 2.3 (9-17)	13.0 ± 2.6 (7.5-17)
Recovery ratio (%)*	68.4 ± 27.3 (0-100)	52.5 ± 30.0† (−35.7-100)
Outcome		
Excellent	8 (42.1%)	8 (20%)
Good	9 (47.4%)	19 (47.5%)
Fair	1 (5.3%)	11 (27.5%)
Unchanged	1 (5.3%)	1 (2.5%)
Worsened	0 (0%)	1 (2.5%)

JOA score shown in Table 2.

Excellent: 80% ≤ recovery rate, good: 40% ≤ recovery rate < 80%, fair: 10% ≤ recovery rate < 40%, unchanged: 0% ≤ recovery rate < 10%, worsened: recovery rate < 10%.

*The values are expressed as the mean and standard deviation, with the range in parentheses.

†Statistically different from the data in A-group ($P < 0.05$).

The clinical results of surgery for the A-group and the P-group are shown in Table 3. The mean preoperative JOA score was 8.3 points in the A-group and 8.6 in the P-group, a difference that was not significant ($P = 0.568$). The mean JOA score 1 year after surgery was 14.2 points in the A-group and 13.0 points in the P-group, again a difference that was not significant ($P = 0.087$). However, the mean recovery rate was significantly higher ($P < 0.05$) in the A-group (68.4%) than in the P-group (52.5%), indicating that neurologic recovery was better after ASF than after laminoplasty. Fifteen patients had a recovery rate less than 40%: 2 in the A-group and 13 in the P-group. One laminoplasty patient and none of the ASF patients developed postoperative aggravation of their neurologic status.

Poor Surgical Outcome After Laminoplasty

The 40 P-group subjects were divided into 2 subgroups: a good recovery group comprising patients whose recovery rate was 40% or higher (n = 27) and a poor recovery group comprising patients whose recovery rate was less than 40% (n = 13). Possible factors affecting poor surgical outcome after laminoplasty are shown in Table 4. No significant differences were seen in the preoperative JOA score between the good and poor outcome groups. The age at surgery was significantly higher in the poor outcome group (mean, 68.0 y) than in the good outcome group (mean, 59.9 y) ($P < 0.05$). The duration of symptoms was significantly longer in the poor outcome group (mean, 61.6 mo) than in the good outcome group (mean, 39.9 mo). No significant differences between the subgroups were observed in the OPLL occupation ratio. The change of the cervical lordotic angle after laminoplasty (ΔC2-C7 lordotic angle) was −1.44 degrees in the good outcome group and −4.85 degrees in the poor outcome group ($P < 0.05$), indicating that the decrease of cervical lordosis after laminoplasty caused poor neurologic recovery. The mean range of motion at intervertebral disc level of maximum cord compression was 6.9 degrees in the good recovery group and 10 degrees in the poor outcome group before surgery ($P < 0.05$), and 3.1 degrees in the good recovery group and 7.2 degrees in the poor outcome group after surgery ($P < 0.05$), indicating that preoperative and postoperative segmental mobility was significantly greater in patients who had a poorer neurologic recovery.

CASE PRESENTATION

Case 1

A 68-year-old man presented with bilateral hand clumsiness and a spastic gait. His preoperative JOA score was 6.5 points. Lateral radiographs, computed tomography, and magnetic resonance images demonstrated a C2-C7 OPLL associated with severe compression of the spinal cord anteriorly at C3/4 (Figs. 2A–C). Extension and flexion radiographs showed that the range of motion at C3/4 was 8 degrees, indicating evident intervertebral mobility at the maximum cord compression level (Figs. 2D, E). Posterior surgery was selected, and a C3-C7 laminoplasty was performed. A postoperative radiograph 1 year after surgery demonstrated progression of cervical kyphosis (Fig. 2F), and magnetic resonance images showed persistent anterior impingement of the spinal cord by OPLL (Figs. 2G, H). Postoperatively, the patient had a poor neurologic recovery: his JOA score was 9 points 1 year after surgery, yielding a recovery rate of 21.7%. The patient was not satisfied with his degree of recovery from myelopathy.

DISCUSSION

Tani et al[12] comparatively analyzed the clinical results of 26 patients who underwent microscopic anterior

TABLE 4. Possible Factors Affecting Poor Surgical Outcome After Laminoplasty

Laminoplasty Subgroups	Good Outcome (n = 27) Recovery Rate ≥ 40%	Poor Outcome (n = 13) Recovery Rate < 40%
JOA score (points)*		
Before surgery	8.6 ± 2.7 (2-12)	8.2 ± 1.9 (4-10.5)
After surgery	14.5 ± 1.6 (11.5-17)	10.0 ± 1.5‡ (7.5-12)
Recovery ratio (%)*	68.3 ± 19.2 (40-100)	19.5 ± 19.5‡ (−35.7-38.9)
Age at surgery (y)*	59.9 ± 10.9 (38-77)	68.0 ± 6.4† (59-82)
Duration of symptoms (mo)*	39.9 ± 44.4 (3-136)	61.6 ± 38.3† (13-130)
Occupation ratio of OPLL (%)*	54.8 ± 11.9 (30-72.7)	58.2 ± 18.6 (20-90)
C2-C7 lordotic angle (degree)*		
Before surgery	12.0 ± 8.0 (−3-34)	14.7 ± 9.6 (−6-27)
After surgery	10.6 ± 8.4 (−9-28)	9.9 ± 10.8 (−13-22)
ΔC2-C7 lordotic angle (degree)*	−1.44 ± 6.3 (−16-10)	−4.85 ± 4.4† (−15-0)
Preoperative segmental ROM (degree)*	6.9 ± 4.1 (0-16)	10.0 ± 4.2† (1-17)
Postoperative segmental ROM (degree)*	3.1 ± 2.4 (0-7)	7.2 ± 5.0† (0-15)

JOA score shown in Table 2.

ΔC2-C7 lordotic angle = postoperative C2-C7 lordotic angle − preoperative C2-C7 lordotic angle. Segmental ROM = segmental range of motion (intervertebral disc mobility) at maximum cord compression level.

*The values are expressed as the mean ± standard deviation, with the range in parentheses.

†Statistically different from the data in good outcome group ($P < 0.05$).

‡Statistically different from the data in good outcome group ($P < 0.01$).

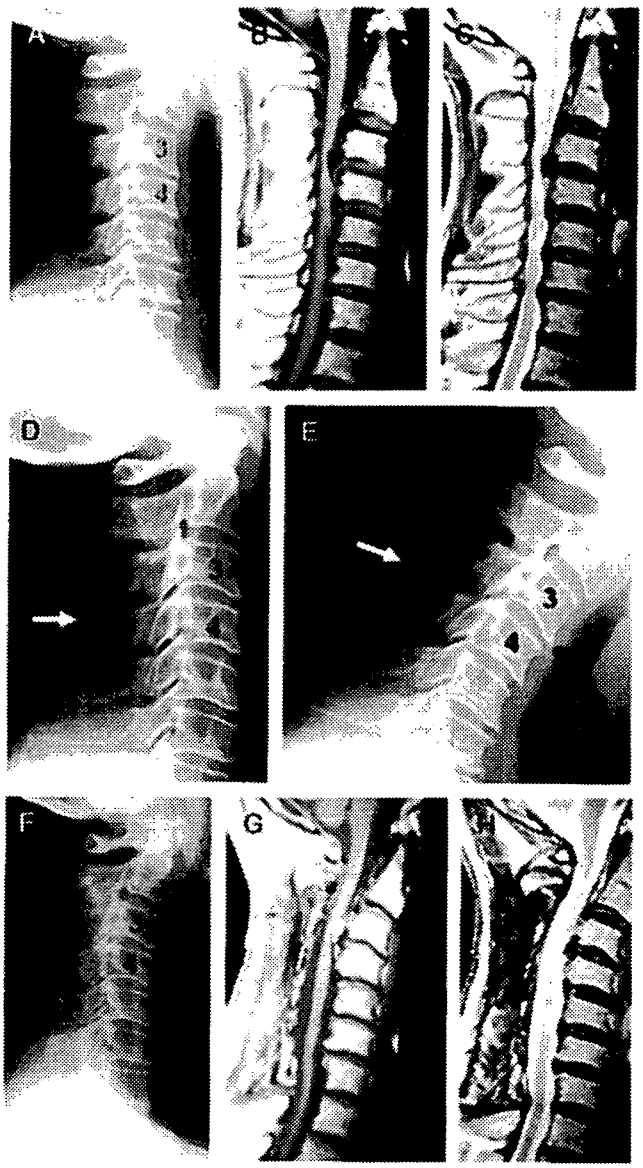

FIGURE 2. A, Preoperative radiographic image at neutral position, (B) T1-weighted midsagittal magnetic resonance (MR) image, and (C) T2-weighted midsagittal MR image of a 68-year-old man (Case 1) demonstrating OPLL at C2-C7 and severe compression of the spinal cord anteriorly at C3/4. D, Preoperative extension radiographic image and (E) flexion radiographic image showing that the range of motion at C3/4 was 8 degrees. Arrows indicate the evident intervertebral disc mobility at C3/4. F, Postoperative radiographic image at neutral position, (G) T1-weighted MR midsagittal image, and (H) T2-weighted midsagittal MR image 1 year after C3-C7 laminoplasty, demonstrating progression of cervical kyphosis and persistent anterior impingement of the spinal cord by OPLL. The recovery rate for this case was 21.7%, representing a poor surgical outcome.

decompression and spinal fusion (n = 14) or laminoplasty (n = 12) for extensive cervical OPLL with an occupation ratio in the spinal canal exceeding 50%. They found that the average recovery rate was significantly higher after anterior surgery than after posterior surgery. No neurologic deterioration occurred after anterior surgery, whereas postoperative neurologic deterioration occurred in 4 patients after posterior surgery. The authors suggested that the following factors affected neurologic deterioration after laminoplasty: (1) decrease in the lordosis of the cervical spine; (2) tethering of nerve roots due to insufficient width for decompression of the spinal cord; (3) inappropriate positioning of the neck during surgery; (4) direct intraoperative damage to the spinal cord; and (5) ischemia of the spinal cord during surgery.

The present study yielded data consistent with those of Tani et al,[12] demonstrating that the surgical outcome of anterior surgery for cervical OPLL was superior to the surgical outcome of posterior surgery. The present results also showed that the decrease of cervical lordosis after laminoplasty caused poor surgical outcome; being principally consistent with the description of Tani et al.[12] In addition, the results demonstrated that elderly patients treated with laminoplasty were especially prone to a poor surgical outcome. Despite the preoperative information they received showing the good surgical outcome associated with anterior surgery, many elderly patients selected posterior surgery. Although they could understand the likelihood of a better neurologic recovery after anterior surgery, these elderly patients judged that the postoperative course of anterior surgery would be too difficult to tolerate.

In the present study, surgical approaches were determined in accordance with the patients' choice. Thus, the study groups were not truly randomized. Despite such limitation of the study design, the present data provided evidence that substantial intervertebral disc mobility at the maximum cord compression level could be a factor causing poor surgical outcome after laminoplasty. The study data demonstrated that the poor outcome group after laminoplasty had larger segmental mobility of vertebrae before surgery and after surgery. We suggest that laminoplasty in patients with massive OPLL may cause insufficient posterior shift of the spinal cord, resulting in persistent anterior impingement of the spinal cord by OPLL. If substantial segmental mobility still remains after surgery in such cases, it is possible that damage to the injured spinal cord progresses.

Based on the present results, we recommend that ASF should be the first choice of treatment for patients with massive OPLL and evident intervertebral disc mobility at the cord compression level. When laminoplasty is selected for such cases, the addition of posterior instrumented fusion would be desirable for stabilizing the spine and decreasing the damage to the cord.

In previous studies, we analyzed factors affecting poor surgical outcomes for thoracic myelopathy due to OPLL. We examined 3 surgical procedures: (1) extirpation of OPLL; (2) posterior decompression alone; and (3) posterior decompression with instrumented fusion. With respect to outcomes, 3 of the 16 patients who underwent posterior decompression alone developed paralysis after

surgery. Two of these 3 postoperative paralysis patients fully recovered after they underwent posterior fixation with instrumentation.[14,15] None of the patients who initially underwent posterior decompression and instrumented fusion for thoracic OPLL developed postoperative paralysis, and all of these patients experienced neurologic recovery despite anterior impingement of OPLL on the spinal cord.[16] These findings suggested that the addition of instrumented fixation reduced the mobility of the spine and prevented damage to the spinal cord. Because most cases of cervical OPLL are associated with a lordotic alignment of the cervical spine, the surgical approach to cervical OPLL will usually differ from the approach to thoracic OPLL. In cervical OPLL patients who have massive OPLL and evident intervertebral disc mobility at the cord compression level, however, our experience with the treatment of thoracic OPLL indicates the potential use of posterior instrumented fusion. In 2003, we began to employ posterior decompression with instrumented fusion as a surgical procedure for elderly patients with cervical OPLL, and thus far have obtained better surgical outcomes from this procedure than from laminoplasty (to be published elsewhere).

REFERENCES

1. Tsuyama N. Ossification of the posterior longitudinal ligament of the spine. *Clin Orthop.* 1984;184:71–84.
2. Hirabayashi K, Miyakawa J, Satomi K, et al. Operative results and postoperative progression of ossification among patients with ossification of cervical posterior longitudinal ligament. *Spine.* 1981;6:354–364.
3. Itoh T, Tsuji H. Technical improvements and results of laminoplasty for compressive myelopathy in the cervical spine. *Spine.* 1985;10: 729–736.
4. Wan-Chun C, Chen-Nen C, Tai-Ngar L, et al. Surgical treatment for ossification of the posterior longitudinal ligament of the cervical spine. *Surg Neurol.* 1994;41:90–97.
5. Kawano H, Handa Y, Ishii H, et al. Surgical treatment for ossification of the posterior longitudinal ligament of the cervical spine. *J Spinal Disord.* 1995;8:145–150.
6. Goto S, Kita T. Long-term follow-up evaluation of surgery for ossification of the posterior longitudinal ligament. *Spine.* 1995; 20:2247–2256.
7. Yamaura I, Kurosa Y, Matsuoka T, et al. Anterior floating method for cervical myelopathy caused by ossification of the posterior longitudinal ligament. *Clin Orthop.* 1999;359:27–34.
8. Sodeyama T, Goto S, Mochizuki M, et al. Effect of decompression enlargement laminoplasty for posterior shifting of the spinal cord. *Spine.* 1999;24:1527–1531.
9. Chiba K, Toyama Y, Watanabe M, et al. Impact of longitudinal distance of the cervical spine on the results of expansive open-door laminoplasty. *Spine.* 2000;25:2893–2898.
10. Matsuoka T, Yamaura I, Kurosa Y, et al. Long-term results of the anterior floating method for cervical myelopathy caused by ossification of the posterior longitudinal ligament. *Spine.* 2001; 26:241–248.
11. Iwasaki M, Kawaguchi Y, Kimura T, et al. Long-term results of expansive laminoplasty for ossification of the posterior longitudinal ligament of the cervical spine: more than 10 years follow up. *J Neurosurg.* 2002;96:180–189.
12. Tani T, Ushida T, Ishida K, et al. Relative safety of anterior microsurgical decompression versus laminoplasty for cervical myelopathy with a massive ossified posterior longitudinal ligament. *Spine.* 2002;27:2491–2498.
13. Ogawa Y, Toyama Y, Chiba K, et al. Long-term results of expansive open-door laminoplasty for ossification of the posterior longitudinal ligament of the cervical spine. *J Neurosurg Spine.* 2004;1:168–174.
14. Yamazaki M, Okawa A, Koda M, et al. Transient paraparesis after laminectomy for thoracic myelopathy due to ossification of the posterior longitudinal ligament: a case report. *Spine.* 2005;30: E343–E346.
15. Yamazaki M, Koda M, Okawa A, et al. Transient paraparesis after laminectomy for thoracic ossification of the posterior longitudinal ligament and ossification of the ligamentum flavum. *Spinal Cord.* 2006;44:130–134.
16. Yamazaki M, Mochizuki M, Ikeda Y, et al. Clinical results of surgery for thoracic myelopathy due to ossification of the posterior longitudinal ligament: operative indication of posterior decompression with instrumented fusion. *Spine.* 2006;31:1452–1460.

Spinal Cord (2007) 45, 250–253

www.nature.com/sc

Case Report

Usefulness of three-dimensional full-scale modeling of surgery for a giant cell tumor of the cervical spine

M Yamazaki*[,1], T Akazawa[1], A Okawa[1] and M Koda[1]

[1]*Department of Orthopaedic Surgery, Chiba University Graduate School of Medicine, Chuo-ku, Chiba Japan*

Study design: Case report.
Objectives: To report a case with giant cell tumor (GCT) of C6 vertebra, in which three-dimensional (3-D) full-scale modeling of the cervical spine was useful for preoperative planning and intraoperative navigation.
Setting: A university hospital in Japan.
Case report: A 27-year-old man with a GCT involving the C6 vertebra presented with severe neck pain. The C6 vertebra was collapsed and the tumor had infiltrated around both vertebral arteries (VAs). A single-stage operation combining anterior and posterior surgical procedures was scheduled to resect the tumor and stabilize the spine. To evaluate the anatomic structures within the surgical fields, we produced a 3-D full-scale model from the computed tomography angiography data. The 3-D full-scale model clearly showed the relationships between the destroyed C6 vertebra and the deviations in the courses of both VAs. Using the model, we were able to identify the anatomic landmarks around the VAs during anterior surgery and to successfully resect the tumor. During the posterior surgery, we were able to determine accurate starting points for the pedicle screws. Anterior iliac bone graft from C5 to C7 and posterior fixation with a rod and screw system from C4 to T2 were performed without any complications. Postoperatively, the patient experienced relief of his neck pain.
Conclusion: The 3-D full-scale model was useful for simultaneously evaluating the destruction of the vertebral bony structures and the deviations in the courses of the VAs during surgery for GCT involving the cervical spine.
Spinal Cord (2007) **45,** 250–253. doi:10.1038/sj.sc.3101959; published online 11 July 2006

Keywords: giant cell tumor; cervical spine; vertebral artery; three-dimensional full-scale model; rapid prototyping

Introduction

Although giant cell tumors (GCTs) of bone have a benign histology, they are locally aggressive tumors. GCT rarely arises in the spine; only 1.3–2.9% of all GCTs of bone involve vertebra above the sacrum.[1,2] Surgical treatment for GCT involving the vertebral column has been considered highly dangerous because of the presence of neurovascular structures. Previous reports have indicated that wide and complete excision of spinal GCTs is often difficult and that the recurrence rate following surgery is 11–42%.[1,3,4]

Among the GCTs involving the spine, complete removal of the tumor from the cervical spine is particularly challenging if a vertebral artery (VA) lies close to the neoplasm. Anterior tumor resection from the cervical spine is generally difficult because vertebral bodies are frequently collapsed by infiltrating tumor, and anatomical landmarks in the operative fields are often difficult to identify. In several reported cases of GCT involving the cervical spine, the authors decided against total excision of the tumor owing to the potential risk of VA injury.[5,6]

In the present report, we describe our experience with surgical treatment of a patient with a GCT involving the C6 vertebra. Before the surgery, we produced a three-dimensional (3-D) full-scale model of the cervical spine from the computed tomography (CT) angiography data using the rapid prototyping (RP) technique. The model clearly showed the anatomical relationship between the destroyed vertebral bony structures and deviations in the paths of the VAs. This information greatly assisted our efforts to excise the tumor and stabilize the spine.

*Correspondence: M Yamazaki, Department of Orthopaedic Surgery, Chiba University Graduate School of Medicine, 1-8-1 Inohana, Chuo-ku, Chiba 260-8677, Japan

Case report

A 27-year-old man was admitted to our hospital with neck pain of 6 months duration. Four months previously, after his neck pain increased in the absence of trauma, the patient consulted doctors at another hospital. Radiological examination revealed that he had a fracture of the C6 vertebra, and additional CT examination suggested that the fracture might be pathological. A needle biopsy established a diagnosis of GCT. The patient underwent selective arterial embolization of the tumor as an alternative to surgery. Following the third embolization, which was performed 2 months before his admission to our hospital, the patient felt severe pain in his upper and lower extremities accompanied by motor weakness in his left leg and sensory loss in his right trunk and leg. His motor weakness gradually recovered, but the patient refused further embolization treatments and was referred to our hospital for surgical treatment of the tumor.

On admission, the patient had severe neck pain and needed a Philadelphia collar for sitting. Hypalgesia was present in the right trunk and leg below the level of the T1 segment. Muscle power was almost normal. Deep tendon reflexes were increased in his lower extremities, and he had a spastic gait.

Cervical spine radiographs showed a pathological fracture of C6. Mid-sagittal reconstruction of the CT images showed that almost all areas of the C6 vertebral body were osteolytic (Figure 1). Axial CT images at the C6 pedicle level showed bilateral destruction of the transverse foramina (Figure 1) and tumor infiltration into the left C6 pedicle and lamina (Figure 1, arrow). Enhanced CT showed that the tumor had also infiltrated around both VAs and that both VAs were shifted laterally (Figure 1, arrowheads). Magnetic resonance images showed tumor infiltration into the spinal canal and close to the dura mater at the C6 level, but compression of the spinal cord was not seen.

To better evaluate the local anatomical structures in this patient, we produced a 3-D full-scale model of the cervical spine from the CT angiography data using the RP technique, employing the binder jet method.[7] Our 3-D full-scale model clearly showed destruction of the C6 vertebra (Figure 2, asterisk) and the deviations in the courses of both VAs (Figure 2, arrowheads). We then performed a simulation of surgery using this model, inserting pedicle screws at C4, C5, T1 and T2 bilaterally (Figure 3). CT images of the simulated screw insertions showed that the insertion points of the left screws were positioned too far laterally, causing these screws to penetrate the medial wall of the transverse foramen uncomfortably close to the left VA (Figure 3, arrowheads). The results of the surgery simulation demonstrated the necessity of positioning the insertion points of the screws more medially during the actual surgery.

Our resection of the tumor and stabilization of the spine consisted of a single-stage operation combining anterior and posterior surgical procedures. Starting with a posterior approach, we performed a fenestration at the left C6 lamina and excised the tumor around the left C6 nerve root. We then inserted pedicle screws at C4, C5, T1 and T2 and performed a C4-T2 posterior fixation with a screw and rod system, utilizing the results of the surgery simulation to properly locate the insertion points of the screws. We then moved the patient into a supine position. Using an anterior approach, we

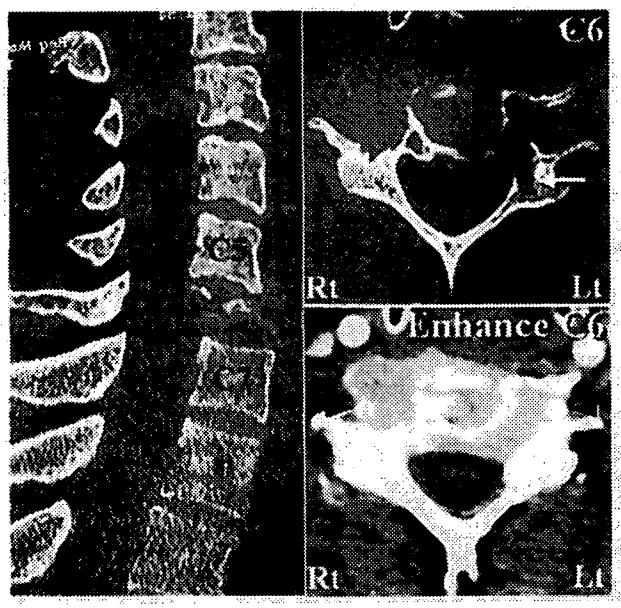

Figure 1 Mid-sagittal reconstruction of a CT image of the cervical spine (left) shows the collapse of the C6 vertebra. CT at the level of the C6 pedicle (right, upper) shows that almost all areas of the C6 vertebral body are osteolytic. The arrow shows tumor infiltration into the left lamina. Enhanced CT at the mid-vertebral level of C6 (right, lower) shows tumor infiltration around both VAs (arrowheads)

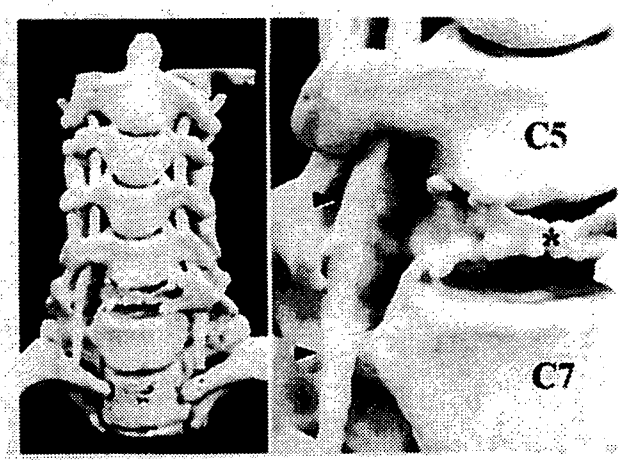

Figure 2 Three-dimensional (3-D) full-scale model of the cervical spine (left) was produced from the CT angiography data. A high-power view of the model (right) clearly shows the collapse of the C6 vertebra (asterisk), destruction of both VA foramina, and a lateral shift of the right VA (arrowheads)

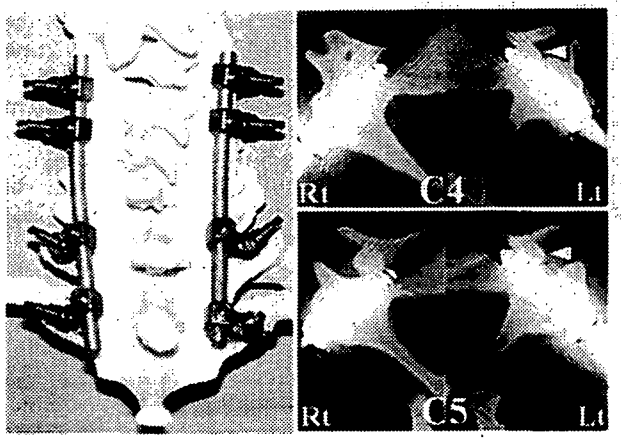

Figure 3 Simulation of surgery was performed using the 3-D full-scale model (left). Pedicle screws were inserted at C4, C5, T1 and T2 and fixed with a 4.75 mm diameter rod. CT images of the model at C4 (right, upper) and C5 (right, lower) levels show the path of the screws. On the left side, the screws were deviated toward the lateral side, penetrating the wall of the transverse foramen uncomfortably close to the left VA (arrowheads)

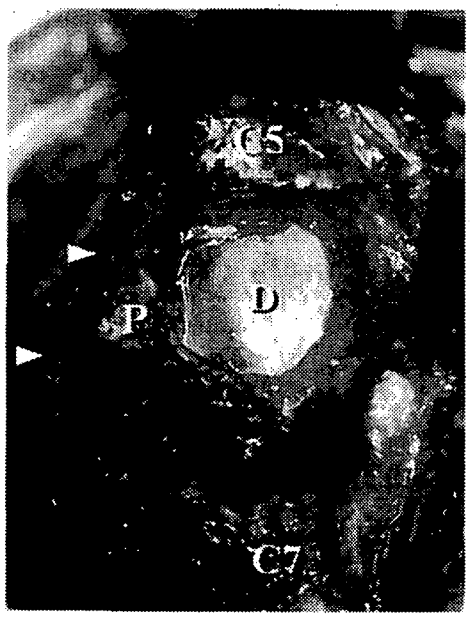

Figure 4 An intraoperative photograph after C6 corpectomy. The inferior third of the C5 vertebra, the superior third of the C7 vertebra and the right C6 pedicel (P) were also excised. The right VA (arrowheads) was exposed, and the tumor was carefully resected to avoid injury to the right VA (D: dura mater)

performed a C6 corpectomy and extirpation of the tumor. Finally, we then performed a C5-C7 fusion using an autograft from the right iliac crest. During the anterior surgery, we were able to identify clearly the VAs and to resect the tumor around the VAs based

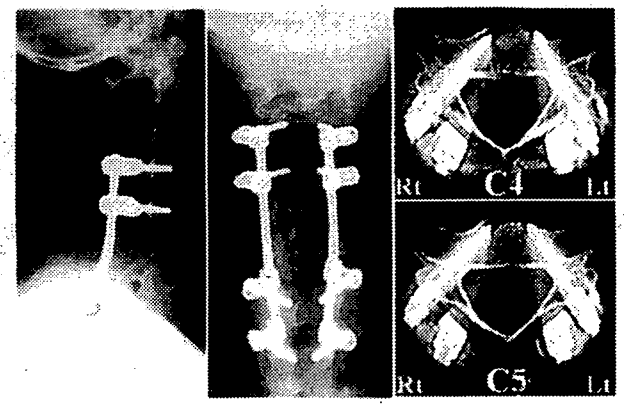

Figure 5 Lateral (left) and anteroposterior (middle) cervical radiographs obtained 6 months after the operation show complete fusion of the autograft at C5–C7. CT images at C4 (right, upper) and C5 (right, lower) pedicle levels show that the pedicle screws are properly positioned

upon the information provided by the 3-D full-scale model (Figure 4). Pathological examination of the extirpated tumor showed multinucleated giant cells and spindle-shaped cells, findings typical of GCT.

Postoperatively, the patient was again fitted with a Philadelphia collar for 3 months, after which time further cervical orthosis was no longer required. After surgery, the patient experienced relief from neck pain, and he returned to work 3 months after surgery. Cervical radiographs 6 months after surgery showed successful C5–C7 fusion (Figure 5) and no evidence of tumor recurrence. CT images at this time showed that the C4 and C5 pedicle screws were properly positioned (Figure 5).

Discussion

RP, a technique initially developed for industrial purposes, is increasingly being utilized in surgical planning. In the field of plastic surgery and craniofacial surgery, RP has been clinically applied to the reconstruction of cranial, mandibular and facial bones.[7] In the field of trauma surgery, Brown *et al*[8] have produced RP 3-D models of multi segmentary acetabular fractures, which they use to simulate fracture reduction and fixation with plate and screws before carrying out these procedures in the operating room. The authors reported that these 3-D models enabled them to easily evaluate the complex structures of fractured bone and to then treat the fractures with improved precision.

In the field of spine surgery, D'Urso *et al*[9] produced 3-D full-scale models from raw CT data for five patients with complex spinal deformities and reported on the usefulness of the models for morphological assessment, intraoperative navigation and rehearsal of surgery. To the best of our knowledge, however, no reports have described 3-D models that can directly evaluate the courses of VAs inside the cervical spine. In the present case, the tumor extended close to the VAs on both sides.

deviating the VA courses laterally, and caused evident destruction of both VA foramina. Anticipating that the detection of VAs within the operative field would be difficult, we produced a 3-D full-scale model from the CT angiography data to simultaneously evaluate the bony structures and the blood vessel courses. Our model clearly showed the relationships between the VAs and the vertebral destruction, facilitating our understanding of the anatomical landmarks around the VAs and thereby enabling us to excise the tumor.

Previously published biomechanical analyses have shown that pedicle screw fixation is the most rigid fixation method of the cervical spine.[10] However, several authors have expressed concern that inserting pedicle screws into the C3–C6 pedicles would be associated with an unacceptable risk of VA injury.[11,12] In a study of their experiences with the insertion of 669 pedicle screws into the cervical spine, Abumi *et al*[10] reported that 45 screws (6.7%) penetrated the pedicle, causing injury to the VA in one patient.

In the present case, we performed simulation of the surgical pedicle screw insertion at C4 and C5 using our 3-D full-scale model. Through this simulation, we were able to determine accurately the starting points for the pedicle screws before the actual surgery, and we did successfully insert the screws. This experience confirmed that simulation of surgery using a 3-D full-scale model can improve the accuracy and safety of reconstructive surgery of the cervical spine.

References

1 Savini R, Gherlinzoni F, Morandi M, Neff JR, Picci P. Surgical treatment of giant-cell tumor of the spine. The experience at the Istituto Ortopedico Rizzoli. *J Bone Joint Surg Am* 1983; **65:** 1283–1289.
2 Goldenberg RR, Campbell CJ, Bonfiglio M. Giant-cell tumor of bone. An analysis of two hundred and eighteen cases. *J Bone Joint Surg Am* 1970; **52:** 619–664.
3 Sanjay BK, Sim FH, Unni KK, McLeod RA, Klassen RA. Giant-cell tumours of the spine. *J Bone Joint Surg Br* 1993; **75:** 148–154.
4 Turcotte RE, Biagini R, Sim FH, Unni KK. Giant cell tumor of the spine and sacrum. *Chir Organi Mov* 1990; **75**(Suppl 1): 104–107.
5 Erdogan B, Volkan Aydin M, Sen O, Sener L, Bal N, Yalcin O. Giant cell tumour of the sixth cervical vertebrae with close relationship to the vertebral artery. *J Clin Neurosci* 2005; **12:** 83–84.
6 Michalowski MB *et al*. Giant cell tumor of cervical spine in an adolescent. *Med Pediatr Oncol* 2003; **41:** 58–62.
7 Ono I, Abe K, Shiotani S, Hirayama Y. Producing a full-scale model from computed tomographic data with the rapid prototyping technique using the binder jet method: a comparison with the laser lithography method using a dry skull. *J Craniofac Surg* 2000; **11:** 527–537.
8 Brown GA, Firoozbakhsh K, DeCoster TA, Reyna Jr JR, Moneim M. Rapid prototyping: the future of trauma surgery? *J Bone Joint Surg Am* 2003; **85**(Suppl 4): 49–55.
9 D'Urso PS *et al*. Spinal biomodeling. *Spine* 1999; **24:** 1247–1251.
10 Abumi K, Shono Y, Ito M, Taneichi H, Kotani Y, Kaneda K. Complications of pedicle screw fixation in reconstructive surgery of the cervical spine. *Spine* 2000; **25:** 962–969.
11 Roy-Camille R, Mazel C, Saillant G, Benazet JP. Rationale and techniques of internal fixation in trauma of the cervical spine. In: Errico T, Bauer RD, Waugh WT (eds). *Spine Trauma*. JB Lippincott: Philadelphia 1991, pp 163–169.
12 Albert TJ, Vacarro A. Postlaminectomy kyphosis. *Spine* 1998; **23:** 2738–2745.

Calcif Tissue Int (2007) 81:132–138
DOI 10.1007/s00223-007-9048-7

Effects of a Single Percutaneous Injection of Basic Fibroblast Growth Factor on the Healing of a Closed Femoral Shaft Fracture in the Rat

Fumitake Nakajima · Arata Nakajima · Akira Ogasawara · Hideshige Moriya · Masashi Yamazaki

Received: 4 March 2007 / Accepted: 5 June 2007 / Published online: 19 July 2007

Abstract Recently, bioactive agents to stimulate bone formation have been available in the orthopedic field. We have shown previously that a single, local injection of basic fibroblast growth factor (bFGF) contributes to the formation of a larger cartilage (soft callus) but does not promote replacement of the cartilage by osseous tissue during experimental closed femoral fracture healing. Aiming at a clinical application, the present study was undertaken to clarify the effects of locally injected bFGF on bone (hard callus) formation and the mechanical properties of the callus in closed fracture healing in rats. Immediately after fracture, a carrier (200 μL of fibrin gel) containing 100 μg of bFGF or carrier alone was applied to the fracture site. At days 42 and 56 postfracture, the bone union rate, bone mineral density (BMD), and mechanical properties (strength and stiffness) of the callus were evaluated. Unexpectedly, with the exception of reduced stiffness in the FGF-injected callus at day 56, none of these parameters showed a significant difference between the control and the FGF-injected groups. Furthermore, the temporal expression pattern of *OPN* mRNA during healing was very similar between groups. We conclude that, in the healing of closed fractures of long bones, administration of bFGF forms a larger callus but does not necessarily accelerate the healing process.

Keywords Basic fibroblast growth factor · Closed fracture · Fracture healing · Osteogenesis · Chondrogenesis

F. Nakajima · A. Nakajima · A. Ogasawara · H. Moriya · M. Yamazaki (✉)
Department of Orthopedic Surgery, Chiba University Graduate School of Medicine, 1-8-1 Inohana, Chuo-ku, Chiba 260-8677, Japan
e-mail: masashiy@faculty.chiba-u.jp

While millions of fractures occur annually and the majority heals satisfactorily, 5–10% go on to delayed union or nonunion. Impaired fracture healing results in pseudoarthrosis or skeletal deformity that may cause functional disability. Not only for the treatment of fracture healing but also for that of substantial bone loss in osteoporosis patients, a bioactive agent to stimulate bone formation is quite important in the orthopedic field.

Among the numerous growth factors intrinsic to the skeletal tissues, basic fibroblast growth factor (bFGF) is known as a potent mitogen for a variety of mesenchymal cells [1]. In skeletal tissues, bFGF is produced by osteoblasts and stored in bone matrix and acts as an autocrine/paracrine factor [2]. Previous *in vitro* studies have shown that bFGF inhibits the differentiation of chondrocytes [3], inhibits the expression of alkaline phosphatase activity [4] as well as the synthesis of type I collagen in osteoblasts [2, 4], and stimulates bone resorption [5]. Thus, bFGF has been recognized as a critical regulator of bone cell function. Moreover, several genetic diseases with abnormalities in bone and cartilage formation, such as achondroplasia and thanatophoric dysplasia type II, have been shown to be due to mutations of genes encoding FGFs or their receptors [6, 7], suggesting the importance of FGFs and their signaling in bone and cartilage formation *in vivo*.

Aiming at a clinical application, many investigators have reported the anabolic effect of local and systemic administration of bFGF on bone formation using animal experimental models. Studies using open osteotomy models showed that local administration of bFGF increased callus size and mechanical strength, suggesting that bFGF can enhance fracture healing [8–12]. However, Bland and colleagues [13], using a rabbit tibial fracture model, reported that neither exogenous acidic FGF (aFGF) nor bFGF had a significant effect on the rate of fracture healing.

Recently, we showed that a single, local injection of bFGF enhanced the proliferation of chondroprogenitor cells in the fracture callus, resulting in a prolonged cartilaginous callus phase [14]. Taking these observations into account, the effects of exogenous bFGF on fracture healing are still equivocal and vary among the fracture models used in an individual experiment. To study further the impact of exogenous bFGF on fracture healing, we employed a standardized closed femoral fracture model in the rat and evaluated the effects of a local, single injection of bFGF on fracture healing, in particular on intramembranous ossification (hard callus formation) and the mechanical properties of the callus.

Materials and Methods

Experimental Animals and Fracture Model

Two-month-old male Sprague-Dawley rats weighing approximately 400 g each were used in this study. A standard closed mid-diaphyseal fracture was produced in the right femur of each rat according to the method of Dr. T. A. Einhorn (Boston University Medical Center, Boston, MA) [15]. Briefly, rats were anesthetized with sodium pentobarbital, and a median parapatellar incision was made at the knee. Next, a Kirschner wire (1.1 mm diameter) was introduced into the intramedullary canal of the right femur. After closure of the incision at the knee joint, a mid-diaphyseal fracture was created with an apparatus composed of a guillotine driven by a dropped weight. Immediately after fracture, 100 μg of recombinant human bFGF (provided by Kaken Pharmaceuticals, Tokyo, Japan) in 200 μL of fibrin gel was injected percutaneously into the fracture site (FGF-injected group $n = 63$). In a control experiment, the carrier (200 μL of fibrin gel) alone was injected (control group $n = 65$). Previous studies have shown that the effect of bFGF on bone formation is dose-dependent [9, 11], and we also demonstrated that 100 μg of bFGF significantly increased the size of calluses, whereas such an increase was not found with 10 μg [14]. Thus, we used 100 μg of bFGF for analyzing the effect of exogenous bFGF on closed fracture healing.

During the experiment, all animals were maintained in cages with free access to food and water. These experimental procedures were approved by the Animal Care and Use Committee of Chiba University.

Radiographic Analyses

When animals killed, radiographs were taken at 7, 14, 28, 46, and 56 days after fracture. To judge bony union, 13–15 calluses of the control and FGF-injected groups were evaluated radiographically at days 42 and 56 postfracture. On radiographic evaluation, four cortices (two on the anteroposterior and two on the lateral radiograph) on each callus were evaluated by at least two different authors (all are orthopedic surgeons), and the fracture callus was defined as a bony union when three of four cortices were bridged.

Bone Mineral Density of the Fracture Callus

The bone mineral density (BMD, g/cm^2) of the fracture callus (six calluses for each group) was measured at days 42 and 56 using a regional high-resolution analysis program for small animals (QDR-1000; Hologic, Waltham, MA), as described previously [16]. In brief, the bone mineral content (BMC) was measured in a 10 mm-high diaphyseal segment (5 mm proximal and 5 mm distal to the fracture line), and BMD was calculated as BMC/two-dimensional femur surface.

Biomechanical Testing

Ultimate load to failure and stiffness of the healing fracture calluses (six calluses for each group) were measured at days 42 and 56 by a three-point bending procedure using a materials testing system (MZ-500D; Maruto, Tokyo, Japan), as described previously [16]. The intramedullary nail was removed, and the fractured femur was placed on two rounded bars, with the fracture line positioned between the bars.

Tissue Preparation

Rats were killed at 4, 7, 14, 21, and 28 days postfracture by intracardiac injection of 4% paraformaldehyde after anesthesia. The fractured femurs were dissected and fixed with 4% paraformaldehyde/0.1 M phosphate-buffered saline (pH 7.4) at 4°C for 24 hours and then decalcified with 0.5 M ethylenediaminetetraacetic acid (EDTA)/0.05 M Tris-HCl (pH 7.6). The decalcified tissues were bisected sagittally in the median plane and embedded in paraffin. Four-micrometer midsagittal sections were mounted on silane-coated slides.

Analysis of Cell Growth Activity in the Periosteal Callus

To evaluate cell growth activity, sections were reacted with a monoclonal antibody (PC-10; Dako, Kyoto, Japan) against proliferating cell nuclear antigen (PCNA), as described previously [14, 16, 17]. The number of PCNA-positive cells in the periosteal callus (at least four calluses for each group) was counted at days 4, 7, and 14 after

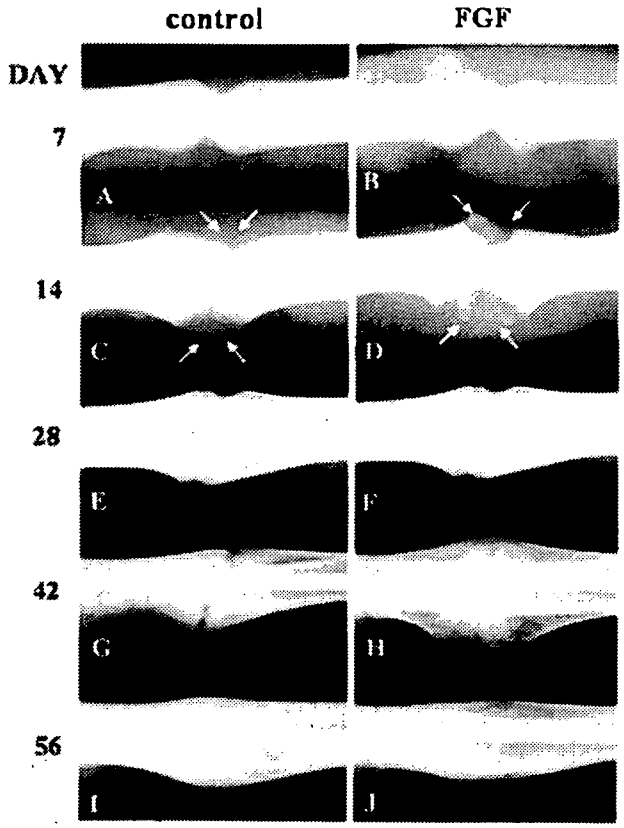

Fig. 1 Radiographic findings for the control (**A, C, E, G, I**) and the FGF-injected (**B, D, F, H, J**) callus during fracture healing. By day 14, bony calluses became evident in both groups but a larger radiolucent area was detected between periosteal calluses in the FGF-injected group compared to the control (**C** and **D**, arrows). At day 42, the size of the FGF-injected callus reached a maximum and was markedly enhanced relative to that of the control (**G, H**)

fracture; and the ratio of PCNA-positive cells to total cells was calculated and expressed as a percentage. The average measurement obtained was used as the PCNA score.

RNA Extraction and Northern Blot Analysis

For RNA extraction, rats were killed after anesthesia with sodium pentobarbital at 4, 7, 14, 21, and 28 days postoperatively. Total cellular RNA was extracted and mixed from at least four calluses for each group at different time points using TRIzol (GIBCO BRL, Rockville, MD) according to the manufacturer's instructions. Ten microgram of total RNA from each day's sample was subjected to 1% agarose gel electrophoresis and transferred to a nylon membrane (Hybond-N; Amersham, Arlington Heights, IL). To evaluate the bFGF-induced mineralization of the callus, the temporal expression of osteopontin (*OPN*) mRNA was quantified. A mouse *OPN* cDNA containing a 1.2 kb fragment was kindly provided by Dr. S. Nomura (Osaka University, Osaka, Japan), and an *OPN* cDNA probe was labeled with ^{32}P using a random priming method. Northern blot analysis was carried out as described previously [14, 16, 17]. The density of each band on the autoradiogram was estimated by an image analyzer (Image Gauge, version 3.1; Fujifilm, Tokyo, Japan).

Table 1 Bone union rate for the control and FGF-injected groups

Union rate (%)	42 days	56 days
Control	6/13 (46.2)	12/15 (80.0)
FGF	8/14 (57.1)	9/13 (69.2)

Statistical Analysis

Differences between groups were determined by analysis of variance. Where differences existed, the Fischer protected least significant difference test was used to determine significance. A value of $P < 0.05$ was considered statistically significant.

Results

Radiographic Findings

In both groups, periosteal callus formation became visible by day 7 after fracture (Fig. 1A,B). By day 14, the size of the bony calluses had increased in both groups; however, a larger radiolucent area was seen between periosteal calluses in the FGF-injected group relative to the control (Fig. 1C,D, arrows), suggesting that exogenous bFGF enhanced cartilage formation. Formation of osseous bridging over the fracture site was completed by day 28 in both groups, and the sizes of the bony calluses in each group were almost equivalent (Fig. 1E,F). At day 42, callus size in the FGF-injected group reached a maximum and was markedly enhanced compared to that of controls (Fig. 1G,H). In both groups, callus remodeling occurred from day 28 and continued up to day 56 (Fig. 1E-J). Finally, we evaluated the rate of bony union at two different time points. At day 42, the union rate of the control and FGF-injected groups was 46.2% and 57.1%, respectively, and at day 56, it was 80.0% and 69.2%, respectively (Table 1).

BMD of the Fracture Callus

In both groups, the BMD of the fracture callus was measured at days 42 and 56 postfracture. The BMD of both groups at day 56 was increased slightly relative to that at day 42 (by 3.6% for each); however, no significant difference was detected between groups at the two different time points (Table 2).

Table 2 BMD of control and FGF-injected calluses (mean ± standard deviation)

BMD (g/cm^2)	42 days	56 days
Control (n = 6)	0.338 ± 0.026	0.350 ± 0.019
FGF (n = 6)	0.337 ± 0.030	0.349 ± 0.012

Table 3 Mechanical strength and stiffness of the control and FGF-injected calluses (mean ± standard deviation)

	42 days	56 days
Strength (n)		
Control (n = 6)	126.5 ± 10.9	239 ± 25.3
FGF (n = 6)	132.7 ± 13.6	234 ± 23.0
Stiffness (n/mm)		
Control (n = 6)	234.4 ± 21.2	357.6 ± 30.6
FGF (n = 6)	251.7 ± 20.7	306.8 ± 28.7*

*Significantly different from control, $P < 0.05$.

Biomechanical Analysis

From day 42 to 56, both the mechanical strength and stiffness of the callus increased markedly in both groups (for strength, by 88% and 76% for the control and FGF-injected groups, respectively; for stiffness, by 53% and 22% for the control and FGF-injected groups, respectively). At day 56, the mechanical stiffness of the FGF-injected group was reduced significantly compared to that of the control; however, no other significant difference was detected between groups at the two different time points (Table 3).

Localization and Quantification of PCNA-Positive Cells in the Periosteal Fracture Callus

In both groups, thickening of the periosteum near the fracture site occurred concurrently with the proliferation of subperiosteal osteoprogenitor cells at day 4 after fracture. In the control group, approximately 15% of the subperiosteal osteoprogenitor cells were PCNA-positive; and in the FGF-injected group, the PCNA score for the osteoprogenitor cells was increased significantly to approximately 30% at this time point (Fig. 2B). At day 7, the PCNA score decreased (12% for the control and 25% for the FGF-injected groups, respectively) in both groups, but the FGF-injected group still showed a significantly increased PCNA score relative to the control (Fig. 2B). In the control group, the PCNA-positive cells were restricted to the subperiosteal osteoprogenitor cells, while they were detected not only in the osteoprogenitor cells but also in the osteoblastic cells around the trabecular bones in the FGF-injected group (Fig. 2A). As fracture healing proceeded, the PCNA score gradually decreased in both groups, with no significant difference being evident at day 14 (Fig. 2B).

Temporal Expression of OPN mRNA in the Fracture Callus

To investigate whether locally applied bFGF could affect mineralization of the fracture callus, we analyzed the temporal expression pattern of *OPN* mRNA and found that it was similar between groups (Fig. 3A,B). In both groups, the expression level increased gradually after fracture and reached a maximum at day 21, when robust mineralization and subsequent bone remodeling were proceeding in the callus. Then, the level of *OPN* mRNA decreased until day 28. There was no significant difference in the expression level of *OPN* mRNA between groups throughout the healing process (Fig. 3B).

Discussion

In the present study, we tested whether a single percutaneous injection of bFGF could accelerate the healing of a closed femoral shaft fracture and observed the effects of this factor, in particular on intramembranous ossification (hard callus formation) and the mechanical properties of the calluses. The results demonstrated that exogenous bFGF increased callus size significantly but not BMD and mechanical properties of the callus.

To explore why exogenous bFGF did not affect mechanical strength of the callus, we investigated whether mineralization and/or remodeling of the callus were altered by the bFGF injection. Both mineralization and remodeling are required for fractured bones to restore strong mechanical properties. Expression of OPN is supposed to reflect mineralization and subsequent bone remodeling during fracture healing, and we demonstrated previously that *OPN* mRNA is expressed strongly in late hypertrophic chondrocytes along the ossification front of the soft callus and in osteoblasts around the trabecular bones of the hard callus [18]. In the present study, we show that exogenous bFGF significantly affected neither expression levels nor a temporal expression pattern for *OPN* mRNA. This could lead to the result that the bFGF injection consequently did not alter the rate of bony union shown in X-ray analysis.

We then asked why exogenous bFGF failed to accelerate fracture healing, although a majority of the previous studies have shown the usefulness of bFGF as a potential agent for accelerating fracture healing. So far, there have been several reports demonstrating that a single, local administration of bFGF increased callus size and mechanical strength in experimental fracture healing [8–12]. In those reports, however, an open osteotomy model, of which conditions

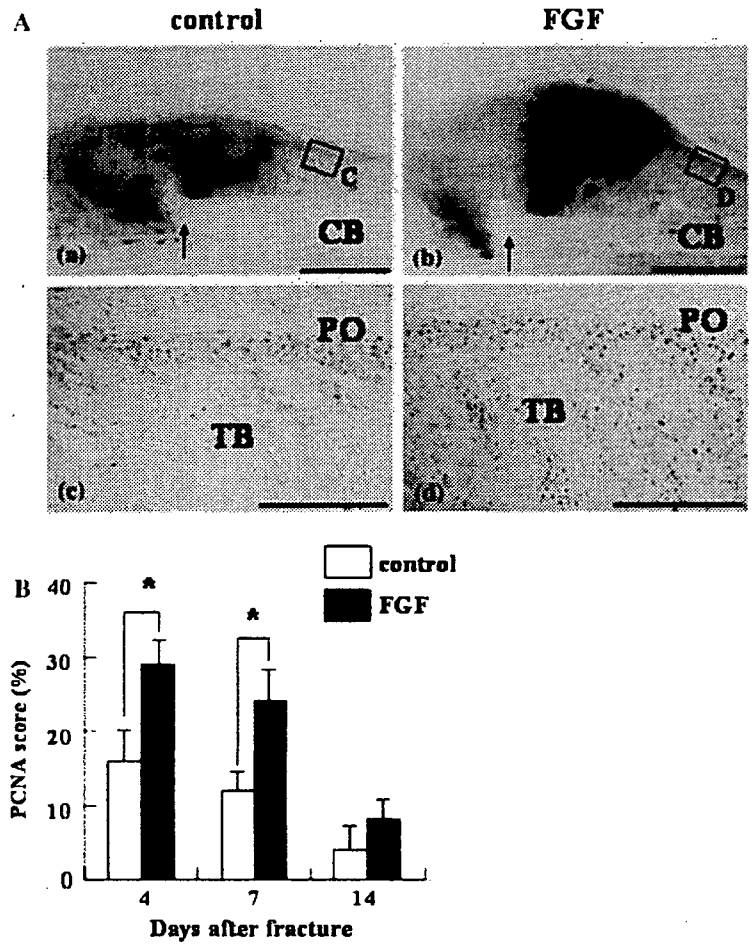

Fig. 2 Localization (**A**) and quantification (**B**) of the PCNA-positive cells in the periosteal callus during intramembranous ossification. (**A**) Panels **a** and **b** show toluidine blue (pH 4.1) staining, and **c** and **d** show immunostaining for PCNA at day 7 after fracture. Areas showing metachromasia in **a** and **b** represent the cartilage area, and boxes in **a** and **b** are enlarged in **c** and **d**, respectively. In the control group, the PCNA-positive cells were restricted to the subperiosteal osteoprogenitor cells (**c**), while they were detected not only in the osteoprogenitor cells but also in the osteoblastic cells around the trabecular bones in the FGF-injected group (**d**). *Arrows* indicate the fracture site. *CB*, cortical bone; *PO*, periosteum; *TB*, trabecular bone. Bars = 500 μm (**a,b**) and 100 μm (**c,d**). (**B**) The PCNA score for the FGF-injected group was increased significantly compared to that for the control in the early stage of healing (days 4 and 7) but not at day 14. Data are expressed as mean ± standard deviation (*significantly different from control, $P < 0.05$)

are totally different from the closed fracture model employed in the present study, was used for an experimental fracture. In an osteotomy model, abundant mesenchymal cells potentially differentiating to chondrocytes should go away from the fracture site. Therefore, locally applied bFGF is likely to selectively stimulate osteoprogenitor cells in the periosteum and enhance intramembranous ossification, by which the hard callus is formed. In contrast, in a closed fracture model, the mesenchymal cells would be left at the fracture site, which contributes to the formation of a larger cartilaginous tissue when bFGF is applied locally. Among the previous studies, Jingushi and colleagues [19] used a rat closed fracture model identical to ours and locally injected aFGF to the fracture site. They showed that aFGF administration markedly enlarged the cartilaginous soft callus but did not increase its mechanical strength, likely supporting our results that exogenous bFGF did not accelerate fracture healing.

The other major difference in the fracture model between ours and other studies is the stability of the fractures. In previous studies by others, fractures were created in non-weight-bearing long bones, such as the fibula or ulna [9–12], or treated either with rigid internal or external fixation when fractures were created in weight-bearing long bones such as the tibia [8, 13]. In the present study, we created a fracture in the mid-shaft of the femur, which is also a weight-bearing bone, but did not treat the fracture with any fixation postoperatively, although a Kirschner wire had been introduced intramedullarly to keep relatively stable mechanical conditions. It has been reported that unstable

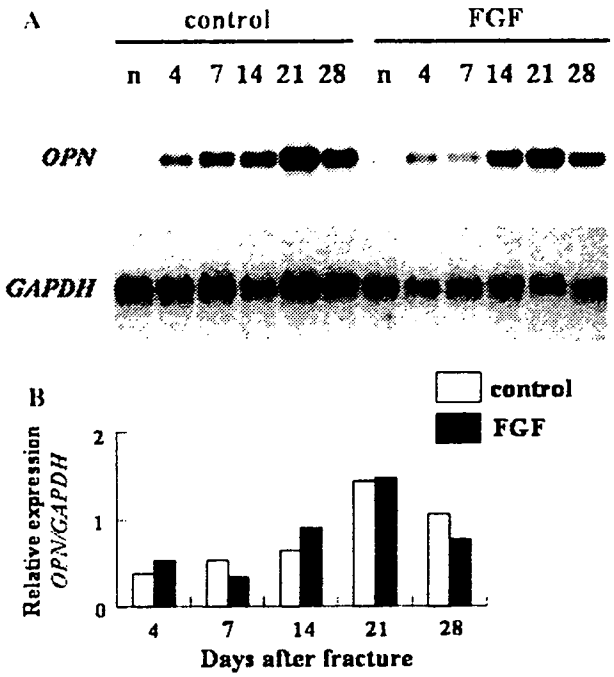

Fig. 3 Northern blot analysis of total RNA from control and FGF-injected calluses. **(A)** Ten micrograms of total RNA from each day's sample was analyzed to quantify the expression level of *OPN* mRNA. Glyceraldehyde-3-phosphate dehydrogenase (*GAPDH*) was used as an internal standard for the amount and integrity of RNA isolation. Representative autographic images are shown. *n*, unfractured femurs; *4*, *7*, *14*, *21*, and *28*, days postfracture. **(B)** Quantification of the expression level of *OPN* mRNA in the control and FGF-injected groups. At least four calluses from each group were mixed and analyzed at different time points. Each band intensity (A) was normalized to the ratio of the internal standard *GAPDH*. There was no significant difference in the expression level between groups throughout the healing process

mechanical conditions enhance chondrogenesis and delay fracture healing [20, 21]. Taken together, these results show that our closed fracture model may be more likely to promote chondrogenesis than other experimental fracture models due to its less rigid mechanical conditions; thus, exogenous bFGF enhanced chondrogenesis (soft callus formation) more than osteogenesis (hard callus formation), as was shown in our previous study [14].

In conclusion, a single, local injection of bFGF increased the size of the callus but not its mechanical properties in the closed fracture healing of the femoral shaft. As a result, exogenous bFGF failed to accelerate the healing process. Although local administration of bFGF could be useful for the treatment of fractures involving bone defects when applied after open reduction and internal fixation, we suggest that bFGF administration alone is not necessarily recommended when the fracture is treated by closed reduction. It should be noted that bFGF peptide has different clinical applications in fracture healing or when used in association with a planned surgical reconstructive procedure.

Acknowledgement We are grateful to Kaken Pharmaceuticals for providing us with recombinant human bFGF. This study was supported by a Grant-in-Aid for Scientific Research from the Ministry of Education, Science and Culture of Japan.

References

1. Rifkin DB, Moscatelli D (1989) Recent developments in the cell biology of basic fibroblast growth factor. J Cell Biol 109:1–6
2. Hurley MM, Abreu C, Gronowicz GA, Kawaguchi H, Lorenzo JA (1994) Expression and regulation of fibroblast growth factor mRNA levels in mouse osteoblastic MC3T3-E1 cells. J Biol Chem 269:9392–9396
3. Wroblewski J, Edwall-Arvidsson C (1995) Inhibitory effects of basic fibroblast growth factor on chondrocyte differentiation. J Bone Miner Res 10:735–742
4. Rodan SB, Wesolowski G, Yoon K, Rodan GA (1989) Opposing effects of fibroblast growth factor and pertussis toxin on alkaline phosphatase, osteopontin, osteocalcin, and type I collagen mRNA levels in ROS 17/2.8 cells. J Biol Chem 264:19934–19941
5. Kawaguchi H, Pilbeam CC, Gronowicz G, Abreu C, Fletcher BS, Herschman HR, Raisz LG, Hurley M (1995) Transcriptional induction of prostaglandin G/H synthase-2 by basic fibroblast growth factor. J Clin Invest 96:923–930
6. Shiang R, Thompson LM, Zhu YZ, Church DM, Fielder TJ, Bocian M, Winokur ST, Wasmuth JJ (1994) Mutations in the transmembrane domain of FGFR3 cause the most common genetic form of dwarfism, achondroplasia. Cell 78:335–342
7. Deng C, Wynshaw-Boris A, Zhou F, Kuo A, Leder P (1996) Fibroblast growth factor receptor 3 is a negative regulator of bone cell growth. Cell 84:911–921
8. Nakamura T, Hara Y, Tagawa M, Tamura M, Yuge T, Fukuda H, Nigi H (1998) Recombinant human basic fibroblast growth factor accelerates fracture healing by enhancing callus remodeling in experimental dog tibial fracture. J Bone Miner Res 13:942–949
9. Radomsky ML, Thompson AY, Spiro RC, Poser JW (1998) Potential role of fibroblast growth factor in enhancement of fracture healing. Clin Orthop 355:S283–293
10. Radomsky ML, Aufdemorte TB, Swain LD, Fox WC, Spiro RC, Poser JW (1999) Novel formulation of fibroblast growth factor-2 in a hyaluronan gel accelerates fracture healing in nonhuman primates. J Orthop Res 17:607–614
11. Kawaguchi H, Kurokawa T, Hanada K, Hiyama Y, Tamura M, Ogata E, Matsumoto T (1994) Stimulation of fracture repair by recombinant human basic fibroblast growth factor in normal and streptozotocin-diabetic rats. Endocrinology 135:774–781
12. Kawaguchi H, Nakamura K, Tabata Y, Ikeda Y, Aoyama I, Anzai J, Nakamura T, Hiyama Y, Tamura M (2001) Acceleration of fracture healing in nonhuman primates by fibroblast growth factor-2. J Clin Endocrinol Metab 86:875–880
13. Bland YS, Critchlow MA, Ashhurst DE (1995) Exogenous fibroblast growth factor-1 and -2 do not accelerate fracture healing in the rabbit. Acta Orthop Scand 66:543–548
14. Nakajima F, Ogasawara A, Goto K, Ninomiya Y, Moriya H, Einhorn TA, Yamazaki M (2001) Spatial and temporal gene expression in chondrogenesis during fracture healing and the effects of basic fibroblast growth factor. J Orthop Res 19:935–944
15. Bonnarens F, Einhorn TA (1984) Production of a standard closed fracture in laboratory animal bone. J Orthop Res 2:97–101
16. Nakajima A, Shimoji N, Shiomi K, Shimizu S, Moriya H, Einhorn TA, Yamazaki M (2002) Mechanisms for the enhancement of fracture healing in rats treated with intermittent low-dose human parathyroid hormone (1–34). J Bone Miner Res 17:2038–2047

17. Nakazawa T, Nakajima A, Shiomi K, Moriya H, Einhorn TA, Yamazaki M (2005) Effects of low-dose, intermittent treatment with recombinant human parathyroid hormone (1–34) on chondrogenesis in a model of experimental fracture healing. Bone 37:711–719
18. Yamazaki M, Nakajima F, Ogasawara A, Moriya H, Majeska RJ, Einhorn TA (1999) Spatial and temporal distribution of CD44 and osteopontin in fracture callus. J Bone Joint Surg Br 81:508–515
19. Jingushi S, Heydemann A, Kana SK, Macey LR, Bolander ME (1990) Acidic fibroblast growth factor (aFGF) injection stimulates cartilage enlargement and inhibits cartilage gene expression in rat fracture healing. J Orthop Res 8:364–371
20. Claes LE, Heigele CA, Neidlinger-Wilke C, Kaspar D, Seidl W, Margevicius KJ, Augat P (1998) Effects of mechanical factors on the fracture healing process. Clin Orthop Relat Res 355:S132–S147
21. Smith-Adaline EA, Volkman SK, Ignelzi MA Jr, Slade J, Platte S, Goldstein SA (2004) Mechanical environment alters tissue formation patterns during fracture repair. J Orthop Res 22:1079–1085